Geosci. Instrum. Method. Data Syst. Discuss., https://doi.org/10.5194/gi-2018-29
Manuscript under review for journal Geosci. Instrum. Method. Data Syst.
Discussion started: 19 June 2018

Geoscientific Instrumentation Methods and Data Systems Discussions
Open Access
EGU

A Hybrid Fluxgate and Search Coil Magnetometer Concept Using a Racetrack Core

David M. Miles[1,2], B. Barry Narod[3], David K. Milling[2], Ian R. Mann[2], David Barona[2], George B. Hospodarsky[1]

[1]Department of Physics and Astronomy, University of Iowa, Iowa City, Iowa, USA
[2]Department of Physics, University of Alberta, Edmonton, Alberta, Canada
[3]Department of Earth, Ocean and Atmospheric Sciences, University of British Columbia, Vancouver, BC, Canada

Correspondence to: David M Miles (david-miles@uiowa.edu)

Abstract.

A proof-of-concept hybrid magnetometer is presented which simultaneously operates as both a fluxgate and a search coil allowing it to sense the magnetic field from DC to two kHz using a single sensor. Historically, such measurements would normally require two dedicated instruments and each would typically require deployment on its own dedicated boom as the instruments mutually interfere. A racetrack fluxgate core combined with a long solenoidal sense winding is shown to be moderately effective as a search coil magnetometer and the search coil effect can be captured without introducing significant hardware complexity beyond what is already present in a typical fluxgate instrument. Several methods of optimizing the search coil action of the hybrid instrument are compared with the best providing sensitivity and noise performance between comparably sized traditional air core and solid core search coil instruments. This hybrid sensor topology should miniaturize to platforms such a CubeSats where multiple boom-mounted instruments are generally impractical so a single hybrid instrument providing modest, but scientifically useful, sensitivity from DC to kHz frequencies would be beneficial.

Geosci. Instrum. Method. Data Syst. Discuss., https://doi.org/10.5194/gi-2018-29
Manuscript under review for journal Geosci. Instrum. Method. Data Syst.
Discussion started: 19 June 2018

Geoscientific Instrumentation Methods and Data Systems Discussions
Open Access
EGU

1 Introduction and Motivation

Space science missions (e.g., Angelopoulos, 2009; Kessel et al., 2013) often need two magnetic field instruments – a search coil magnetometer for high (≥ ~10 Hz) frequencies (Figure 1a) and a fluxgate for the static field and low frequencies (Figure 1b). These two instruments will interfere with each other if they are located too close together. The search coil can detect the drive signal in the fluxgate magnetometer and the ferromagnetic core typically used for magnetic gain in the search coil distorts the field measured by the fluxgate. The two instruments are therefore frequently mounted on separate deployable booms which affect spacecraft control and can impinge in the field of view of other instruments.

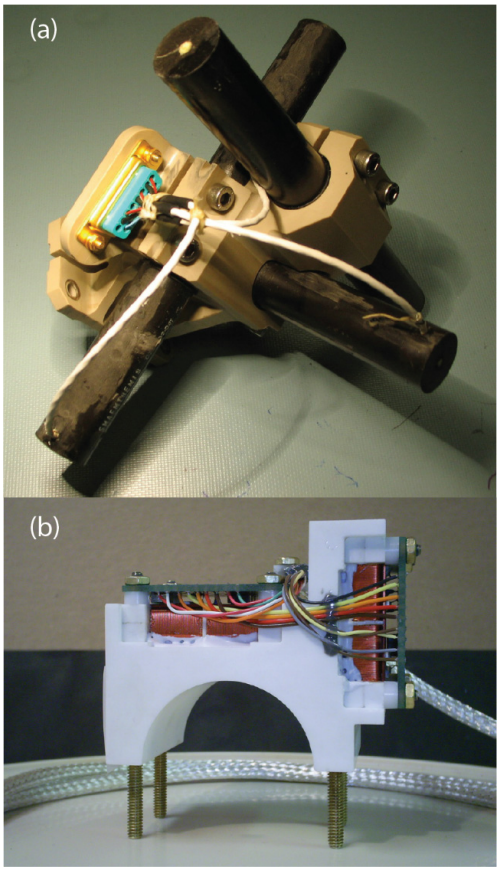

Figure 1: (a) THEMIS search coil showing typical long cylindrical sense coils – credit NASA. (b) Fluxgate sensor showing compact rectangular sense coils – from Wallis et al., (2015).

Search coil magnetometers and fluxgate magnetometers (e.g., reviews by Hospodarsky, 2016; Primdahl, 1979) both sense the local magnetic field through the electromagnetic force (EMF) induced by changing magnetic flux $\boldsymbol{\Phi}$ described by the generalized induction equation (Eq. 1) for a coil of wire of N turns and area $\boldsymbol{A}$, in a field $\boldsymbol{H}$, with a ferromagnetic core of relative permeability, μ_r:

$$V_i = \frac{d}{dt}\boldsymbol{\Phi} = \frac{d}{dt}(N\mu_0\mu_r\boldsymbol{A}\cdot\boldsymbol{H}) \approx (N\mu_0\mu_r\boldsymbol{A})\cdot\frac{d\boldsymbol{H}}{dt} + (N\mu_0\mu_r\boldsymbol{H})\cdot\frac{d\boldsymbol{A}}{dt} + (N\mu_0\boldsymbol{A}\cdot\boldsymbol{H})\frac{d\mu_r}{dt} \quad (1)$$

Geosci. Instrum. Method. Data Syst. Discuss., https://doi.org/10.5194/gi-2018-29
Manuscript under review for journal Geosci. Instrum. Method. Data Syst.
Discussion started: 19 June 2018

Geoscientific Instrumentation Methods and Data Systems Discussions

Search coils measure the voltage induced due to the changing magnetic field ($d\boldsymbol{H}/dt$) while fluxgates measure the voltage induced by changing the relative permeability of a periodically saturating ferromagnetic core ($d\mu_r/dt$). Search coils typically have no single dominant noise source so compact space instruments tend to use a long ferromagnetic core for magnetic gain and tens of thousands of turns of wire to increase sensitivity. Fluxgate noise is typically dominated by the magnetic noise of the ferromagnetic core so only small, compact flat windings of a few hundred turns are required to avoid the coil being a significant noise source. This paper describes a proof of concept hybrid magnetometer which explores if both the search coil and fluxgate sense mechanisms can be simultaneously extracted from a common sense winding.

Several authors (Gordon et al., 1965; Hinnrichs et al., 2000; Ripka, 1990, 1993, 2000) have explored using long racetrack (oval) cores (Figure 2d) instead of circular (Figure 2a) ring-cores. The racetrack geometry mimics the long cylindrical cores often used in search coil sensors (Figure 2c) and is compatible with similar long solenoidal sense windings (Figure 2b). The fluxgate action has been demonstrated to have bandwidth to at least 3 kHz (Ioan et al., 1996; Miles et al., 2013; Primdahl et al., 1994). However, since fluxgate sensitivity is essentially flat with frequency and search coil gain tends to increase with frequency until the self-resonance of the coil, search coil magnetometers tend to provide better sensitivity above a few tens of Hz. Ripka, (1995) investigated whether the feedback coil in a fluxgate could also be used as a search coil magnetometer. This paper extends that concept by changing the geometry of the sensor to mimic that of a search coil and exploring whether the search coil signal extraction can be improved by interleaving its capture with the fluxgate action.

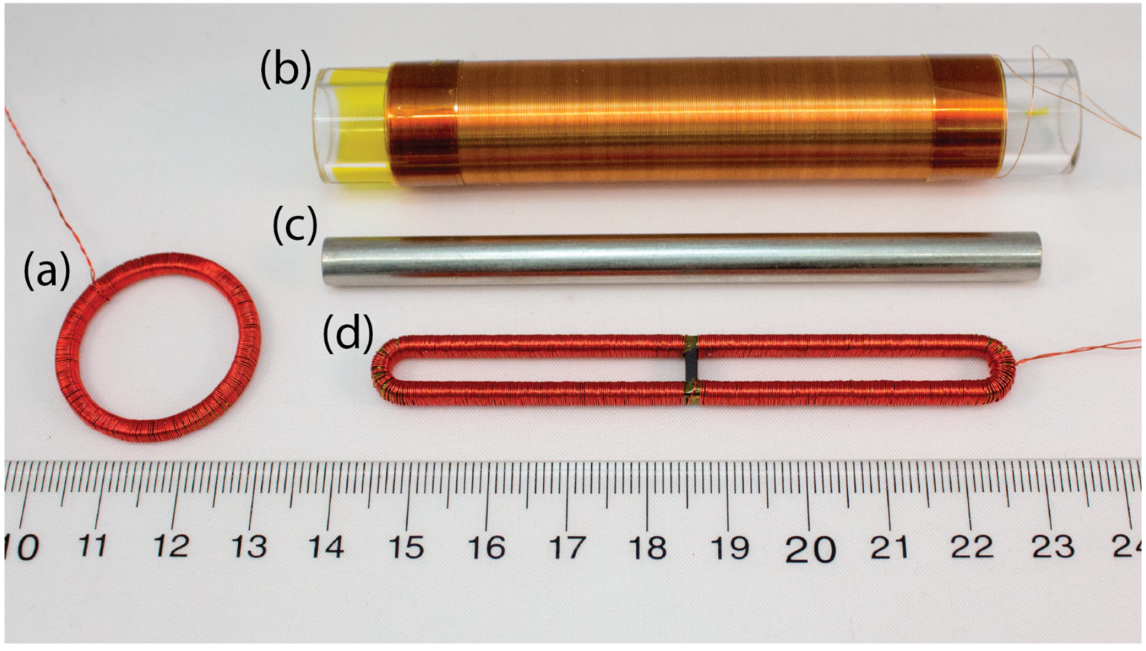

Figure 2: (a) Traditional 25.4 mm fluxgate ringcore. (b) A solenoidal sense winding. (c) Solid Permalloy core representative of search coil magnetometers. (d) Racetrack fluxgate ring core similar in geometry to that used in a search coil.

Geosci. Instrum. Method. Data Syst. Discuss., https://doi.org/10.5194/gi-2018-29
Manuscript under review for journal Geosci. Instrum. Method. Data Syst.
Discussion started: 19 June 2018

Geoscientific Instrumentation Methods and Data Systems Discussions

2 Experimental Hybrid Design

Fluxgate magnetometer cores are periodically driven into magnetic saturation to modulate the local magnetic field. The fluxgate signal is generated by the core's changing permeability as it enters and exits magnetic saturation. However, because the core is typically driven in resonance (Acuna, 1974) with short period, high amplitude current spikes the core is unsaturated about half the time. The solenoidal sense coil should act as a solid-core search coil when the core is unsaturated, an air-core search coil when the core is in saturation, and a fluxgate while the core is entering or leaving saturation. If the saturation of the core and the sampling of the sense coil are synchronized, the different sensor effects should be separable using digital signal processing allowing the sensitivity and noise floor of the two effects to be compared. Utilizing both the search coil and fluxgate mechanisms may provide a way to combine the flat frequency response of the fluxgate with the increasing gain with frequency of the search coil to eventually span a range from DC to >10 kHz in a single instrument.

The racetrack cores presented here were produced as part of a larger project to apply the theory of Narod, (2014) to produce lower noise fluxgate cores and cores in non-traditional sizes and geometries (Miles et al., 2016). Most of that work used 25.4 mm circular ringcore (Figure 2a) but a few racetrack cores (Figure 2d) were manufactured to explore the role of geometry on core noise. The racetrack core is formed on an Inconel bobbin with an 82.5 mm long axis, a 9.65 mm short axis, and a 1.65 mm channel on its outside surface (Figure 3). Three layers of a 100 µm foil are spiral wrapped into the groove and attached with spot welds. The foil was manufactured by successive cold-rolling of a 6.0-81.3 Molybdenum-Nickel Permalloy which was then coated with an insulating layer of magnesium oxide. The assembled bobbin and foil were heat treated for four hours at 1150 °C in a reducing atmosphere of 5% Hydrogen in 95% Argon.

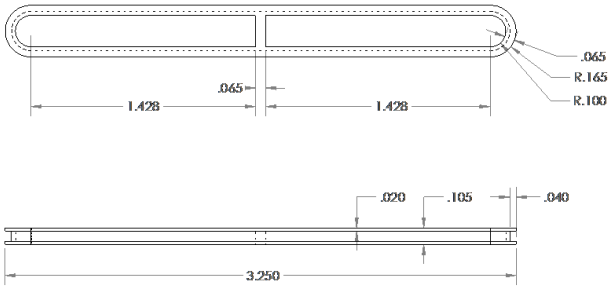

Figure 3: Racetrack foil bobbin used in the magnetometer ringcore for the hybrid magnetometer. Units shown in inches.

The drive winding for the racetrack was 677 turns of AWG 32 enamelled wire wound toroidally. The sense winding was arbitrarily chosen to be 2,247 solenoidal turns of AWG 37 enamelled wire in four layers on fused quartz tube with an outer diameter of 15.4 mm. The length of the solenoidal winding was roughly matched to long axes of the racetrack core. A Permalloy rod of 7 mm diameter and 95 mm length was used to compare the hybrid magnetometer sensitivity to that of the same sense winding operated as a traditional search coil with a solid core.

3 Experimental Setup

Figure 4 shows a block diagram of the setup used to explore the hybrid magnetometer concept. The magnetometer is operated open-loop, without magnetic feedback, to examine the natural response of the sensor. A Field Programmable Gate Array (FPGA)

Geosci. Instrum. Method. Data Syst. Discuss., https://doi.org/10.5194/gi-2018-29
Manuscript under review for journal Geosci. Instrum. Method. Data Syst.
Discussion started: 19 June 2018

Geoscientific Instrumentation Methods and Data Systems Discussions

is used to send 2.5 kHz alternating polarity Power Amplified (PA) current pulses (I_{drive}) into the toroidal drive winding to periodically saturate the racetrack core. The solenoidal sense winding is used in the short-circuit/current-output configuration such that the changing magnetic flux due to the external field (H_{sense}) experienced by the coil induces a current, I_{Sense}. This current is converted to an equivalent voltage (I/V), passed through a weak single-pole low-pass anti-alias filter with a -3 dB point at 5 kHz (LPF) and then synchronously digitised (ADC) in phase with the drive by the FPGA.

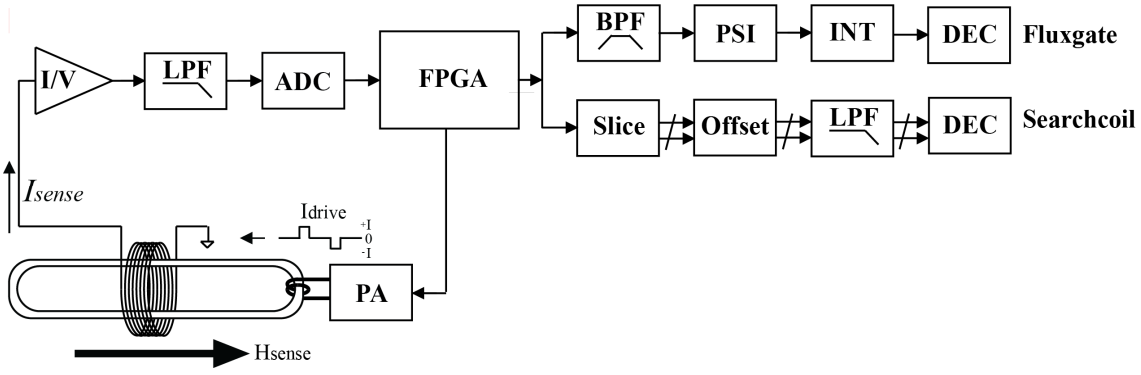

Figure 4: Schematic of test setup showing driven sensor, analog processing, and parallel digital processing paths of common sampled data for fluxgate and search coil reconstruction. Adapted from Miles et al., (2013).

Digital signal processing is used to separate the search coil and fluxgate signals in the raw ADC stream. The fluxgate path follows a classic second harmonic design, the data are band pass filtered (BP) at the second harmonic, run through a phase sensitive inverter (PSI), integrated (INT), and then decimated (DEC) to 400 sps. In the search coil path, the raw data are also sliced into four separate streams corresponding to different phases of the core magnetisation cycles (Slice) and each has a static offset removed (Offset) and is then low-pass filtered (LPF) and decimated (DEC) to 2500 sps search coil data streams.

Figure 5 shows a fast Fourier transform of the raw ADC samples captured from the hybrid sensor driven as a fluxgate and exposed to a 100 nT sinusoidal test signal. The test signal is visible at 100 Hz baseband (Figure 5a) via the search coil action. The fluxgate drive is clear at 2.5 kHz (Figure 5b) and 7.5 kHz (Figure 5d) and fluxgate signal appears at the 5 kHz second harmonic (Figure 5c). The test signal appears in the inset through the fluxgate action as the lower 4.9 kHz (Figure 5e) and upper 5.1 kHz (Figure 5f) sidebands analogous to amplitude modulation radio encoding (Hinnrichs et al., 2001; Miles et al., 2013). All signals are well separated in frequency space suggesting that they can likely be isolated and reconstructed using a low-pass filter (red) for the search coil effect and a band-pass filter (green) for the fluxgate.

Geosci. Instrum. Method. Data Syst. Discuss., https://doi.org/10.5194/gi-2018-29
Manuscript under review for journal Geosci. Instrum. Method. Data Syst.
Discussion started: 19 June 2018

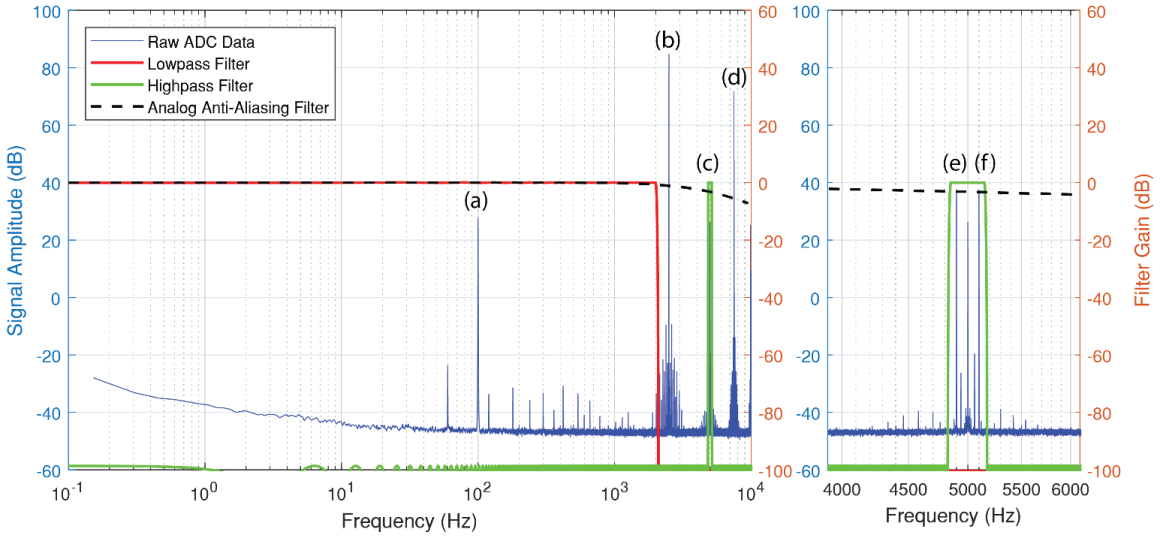

Figure 5: Fast Fourier transform of raw ADC data with 100 nT 100 Hz magnetic test signal. (a) Baseband test signal at 100 Hz. Fluxgate drive signal at (b) 2,500 Hz and (d) 7,500 Hz (c) Second harmonic fluxgate signal at 5,000 Hz. Fluxgate signal sidebands at (e) 4,900 and (f) 5,100 Hz. Note that all signals are well separated in frequency space.

4 Driving and Digitising the Sensor

The racetrack core was driven at 2.5 kHz using the resonant drive circuit described in Miles et al., (2016). The current circulating in the toroidal drive winding was measured using a 0.1 Ohm current snoop resistor and is shown in Figure 6a. Note that, due to the tuning of the resonant drive circuit, the current pulses are engineered to have a high amplitude capable of pushing the racetrack core into deep magnetic saturation but have a short duration. This low duty-cycle reduces power consumption and has the core in deep saturation less than 25% of the time. The current output of the sense winding, transformed into an equivalent voltage and anti-alias filtered, is shown in Figure 6b. Figure 6a/b were captured at high cadence using a benchtop oscilloscope. The phase offset between the drive current pulses (Figure 6a) and the sensor output waveform (Figure 6b) is believed to result from the RLC behaviour of the sense coil and preamp.

Geosci. Instrum. Method. Data Syst. Discuss., https://doi.org/10.5194/gi-2018-29
Manuscript under review for journal Geosci. Instrum. Method. Data Syst.
Discussion started: 19 June 2018

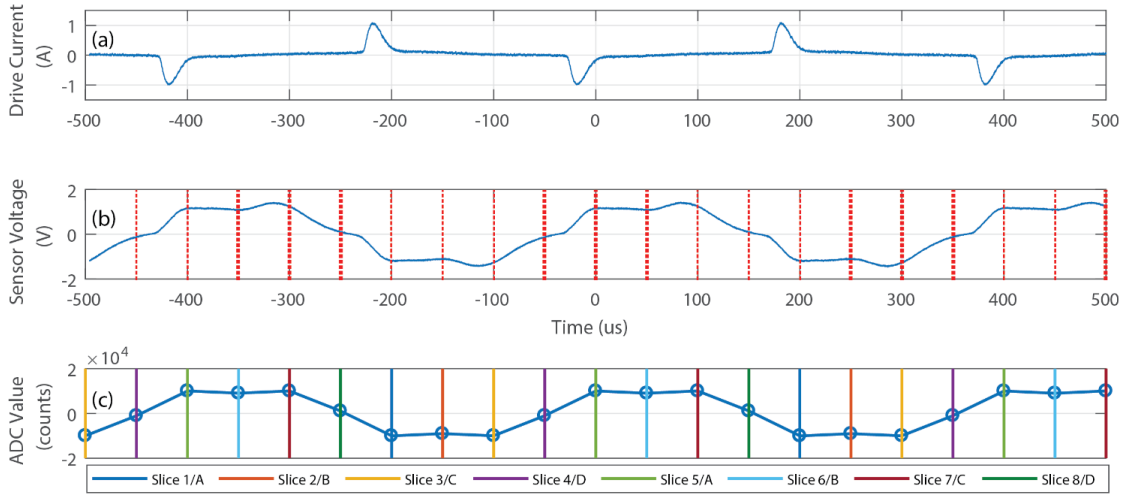

Figure 6: (top) Drive current into the racetrack ringcore. (middle) Analog output of the long solenoidal sense winding and ADC sampling points. (bottom) Digitised sensor output with eight colour coded phase 'slices'.

An equivalent representative time series, captured through the ADC, is shown in Figure 6c. The ADC samples at 20,000 sps or four times faster than required for a classic second harmonic direct digitised fluxgate. The vertical lines show the trigger points of the ADC and are colour coded to indicate how the data are 'sliced' into eight time series corresponding to the eight different phases in the magnetisation loop of the core. Samples contemporaneous with the current pulses correspond to the interval when the core is in deep magnetic saturation during which time the sensor should function like an air core search coil. Equidistant between the current pulses the core should be unsaturated and the sensor should function like a traditional high permeability core search coil albeit with an unusually low-mass core. Between these extremes the core is likely partially saturated. This stream of raw samples will be reconstructed as both a fluxgate and search coil magnetometer below.

Figure 7 shows the power spectral density (PSD) of the ADC stream with a 100 nT sinusoid at 100 Hz applied to the sensor. Black shows the all ADC samples and the colours show demodulation into eight separate streams corresponding to Slice 1-8 in Figure 6 and the eight phases of the ringcore magnetisation cycle.

Geosci. Instrum. Method. Data Syst. Discuss., https://doi.org/10.5194/gi-2018-29
Manuscript under review for journal Geosci. Instrum. Method. Data Syst.
Discussion started: 19 June 2018

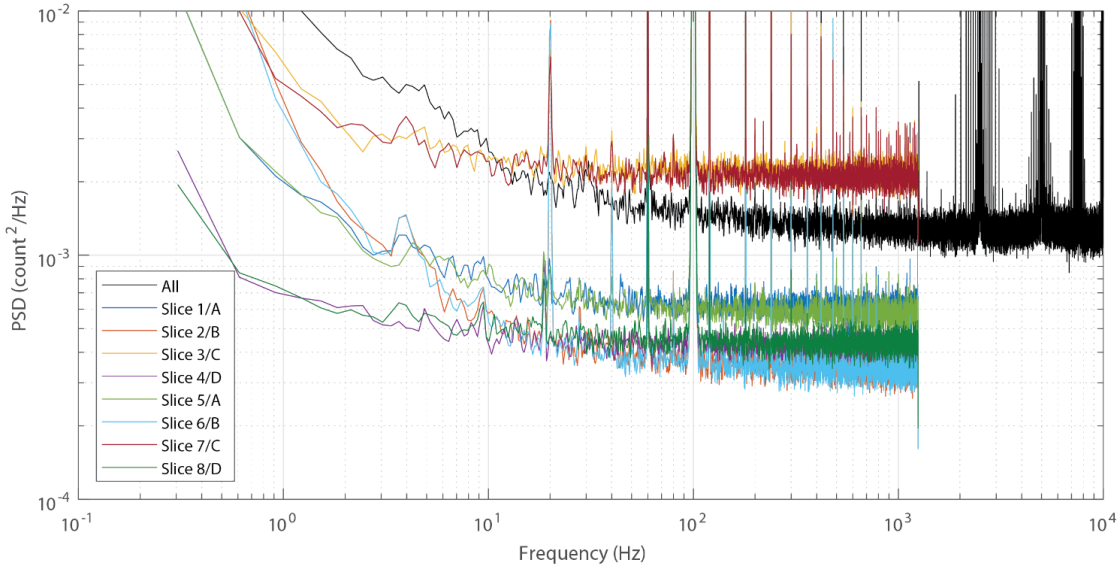

Figure 7: Power Spectral Density (PSD) of the raw ADC values (black) and demodulated into eight slices (colours) corresponding to the eight phases of the ringcore magnetisation cycle.

The nine spectra have been normalised such that the 100 Hz test signal has a common amplitude. As expected, the eight slices form four pairs corresponding to the equivalent places in the positive and negative phases of the drive signal. For the remainder of this manuscript the data will be sliced into four streams made up as A (Slice 1 and 5), B (Slice 2 and 6), C (Slice 3 and 7) and D (Slice 4 and 8).

5 Fluxgate Reconstruction

Figure 8 shows the steps in reconstructing the fluxgate signal. The fluxgate action acts analogous to Amplitude Modulation (AM) radio encoding. A natural signal at frequency f_o is modulated to two sidebands around the second harmonic of the drive signal $2f \pm f_o$. The raw ADC samples (Figure 8a) are therefore band pass filtered (Figure 8b) at the second harmonic of the drive plus or minus the desired bandwidth of the fluxgate path (5,000 +/- 150 Hz) to isolate the fluxgate signal from the search coil signal at baseband and the harmonics of the drive signal (2,500 and 5,000 Hz respectively).

Geosci. Instrum. Method. Data Syst. Discuss., https://doi.org/10.5194/gi-2018-29
Manuscript under review for journal Geosci. Instrum. Method. Data Syst.
Discussion started: 19 June 2018

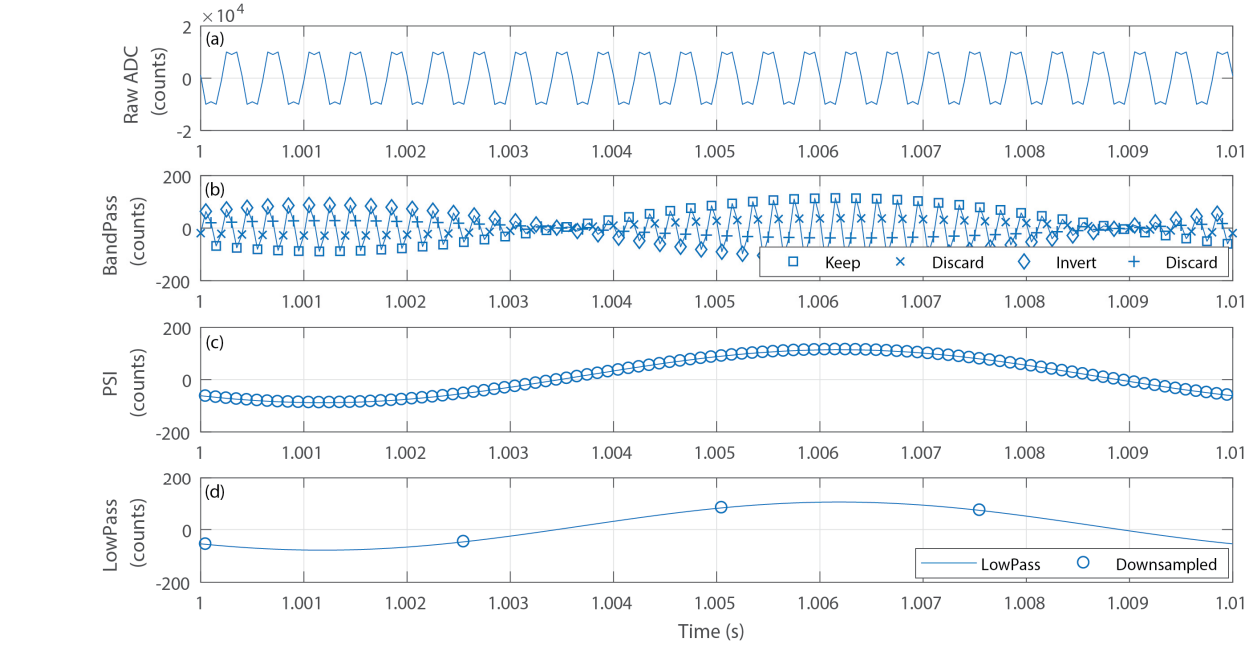

Figure 8: (a) Raw ADC samples. (b) Band-pass filtered samples showing which samples are kept, inverted and dropped in the phase sensitive inverter. (c) Reconstructed test signal. (d) Averaged and decimated fluxgate stream.

The band-pass filtered data (Figure 8b) manifest the 100 Hz magnetic test signal as the envelope of the 5 kHz (2f) oscillation. This is demodulated as marked in Figure 8b. Every other extremum point is inverted and the intermediary points are discarded. The intermediary points can be inverted and included, although they introduce a significant 2f oscillation. However, doing so was found to decrease the signal to noise ratio. The phase sensitive inversion restores the sinusoidal test signal (Figure 8c) which is then averaged and decimated to produce a 400 sps fluxgate stream shown as the circles in Figure 8d.

Figure 9a shows that the sensitivity of the fluxgate path varies by less than 0.5 dB from DC to 100 Hz (normalised to 0 dB at DC).

Geosci. Instrum. Method. Data Syst. Discuss., https://doi.org/10.5194/gi-2018-29
Manuscript under review for journal Geosci. Instrum. Method. Data Syst.
Discussion started: 19 June 2018

Geoscientific Instrumentation Methods and Data Systems Discussions
Open Access
EGU

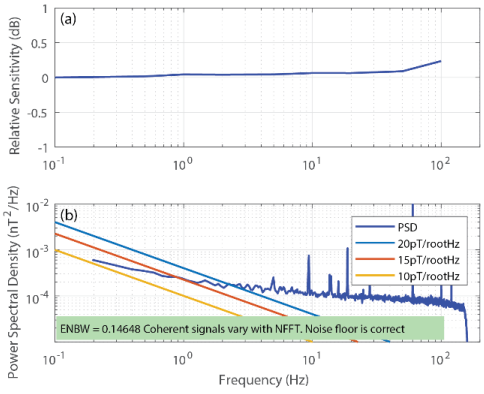

Figure 9: (a) Variation of the fluxgate sensitivity with frequency. (b) Power spectral density (PSD) noise floor of the fluxgate path showing ~15 pT Hz$^{-1/2}$ at 1 Hz.

Figure 9b shows the Power Spectral Density (PSD) noise floor of the fluxgate path calculated with data taken while the sensor was in a three layer mumetal magnetic shield. The core achieves a modest ~15 pT Hz$^{-1/2}$ at 1 Hz. The same foil in roughly the same quantity with the same heat treatment achieves ~6 pT Hz$^{-1/2}$ at 1 Hz when wound onto a 25.4 mm circular ringcore suggesting that something about the manufacture or drive of the racetrack core is not yet optimised. This is beyond the scope of this manuscript and is the subject of ongoing work.

6 Search coil Path

Figure 10 shows the steps in the reconstruction of the search coil signals. The raw ADC values (Figure 10a) are low pass filtered at 1,000 Hz to remove the fluxgate drive and modulation creating the 'All Samples' trace in Figure 10b and then decimated (Figure 10c). The raw ADC Samples are also sliced into four time series (Slice A-D) corresponding to the four phases of the magnetisation cycle of the core, low pass filtered at 1,000 Hz to remove the second harmonic modulation, and independently detrended to remove the static offset caused by that phase of the magnetisation cycle (Figure 10b).

Geosci. Instrum. Method. Data Syst. Discuss., https://doi.org/10.5194/gi-2018-29
Manuscript under review for journal Geosci. Instrum. Method. Data Syst.
Discussion started: 19 June 2018

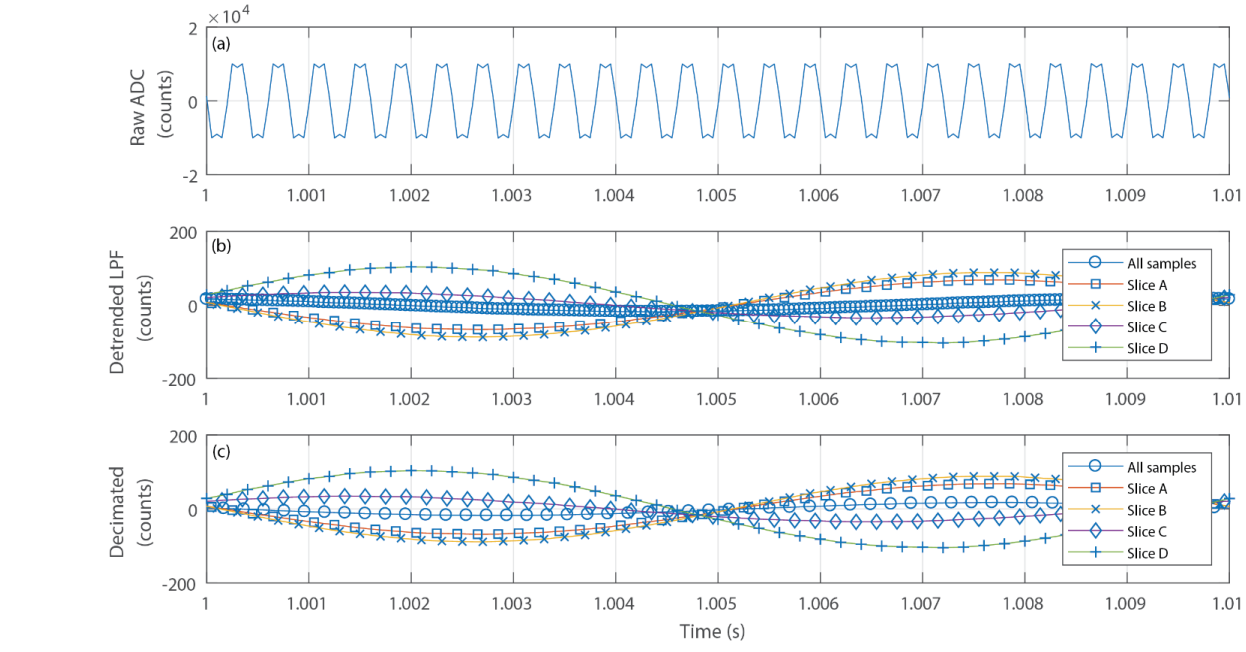

Figure 10: Reconstruction of the search coil signal from (a) raw ADC data to (b) sliced, low pass filtered, and detrended and (c) decimated to common cadence.

The five time series show the 100 Hz magnetic test signal at significantly different amplitudes. This is consistent with the general trend shown Figure 7 where each digitisation offset captures a different degree of core saturation and hence a different magnetic gain. Figure 11a compares the sensitivity (nT/bit) as a function of frequency for each of the hybrid search coil time series and for the same sense coil used as a traditional search coil. The sense coil was operated as an air core, with a solid mumetal core, and with the racetrack core in unsaturated and continually saturated states. As expected, all configurations perform similarly above ~2 kHz where the coil is expected to dominate. At lower frequencies, the effect of the magnetic gain of the core becomes more significant and, below ~100 Hz, the gain of the five hybrid search coil traces becomes unexpectedly flat with frequency.

Between ~200 Hz and ~2,000 Hz the ordering and trend of the sensitivities matches intuitive expectations. The air core and the continually saturated racetrack core provide comparable gain. At the other extreme, the unsaturated racetrack provides about half the gain of the solid mumetal rod. The five hybrid search coil reconstructions lie between these with the unsliced data providing the lowest sensitivity.

The constant gain below ~40 Hz for the hybrid search coil reconstructions appears to be a frequency folding effect caused by insufficient antialiasing before digitisation. The ringcore is driven at 2,500 Hz so the fluxgate modulation will manifest as sidebands around the even harmonics at 5,000, 10,000, 20,000 Hz, etc. A 1 Hz magnetic test signal will therefore create a sideband at 20,001 Hz (eight harmonic). The sensor is sampled at 20,000 sps creating a 10,000 Hz Nyquist frequency. Therefore, the 20,001 Hz sideband will frequency fold over the Nyquist frequency and 0 Hz down to an aliased 1 Hz which will dominate compared to the small sensitivity of the search coil at low frequencies.

Geosci. Instrum. Method. Data Syst. Discuss., https://doi.org/10.5194/gi-2018-29
Manuscript under review for journal Geosci. Instrum. Method. Data Syst.
Discussion started: 19 June 2018

Geoscientific Instrumentation Methods and Data Systems Discussions
Open Access
EGU

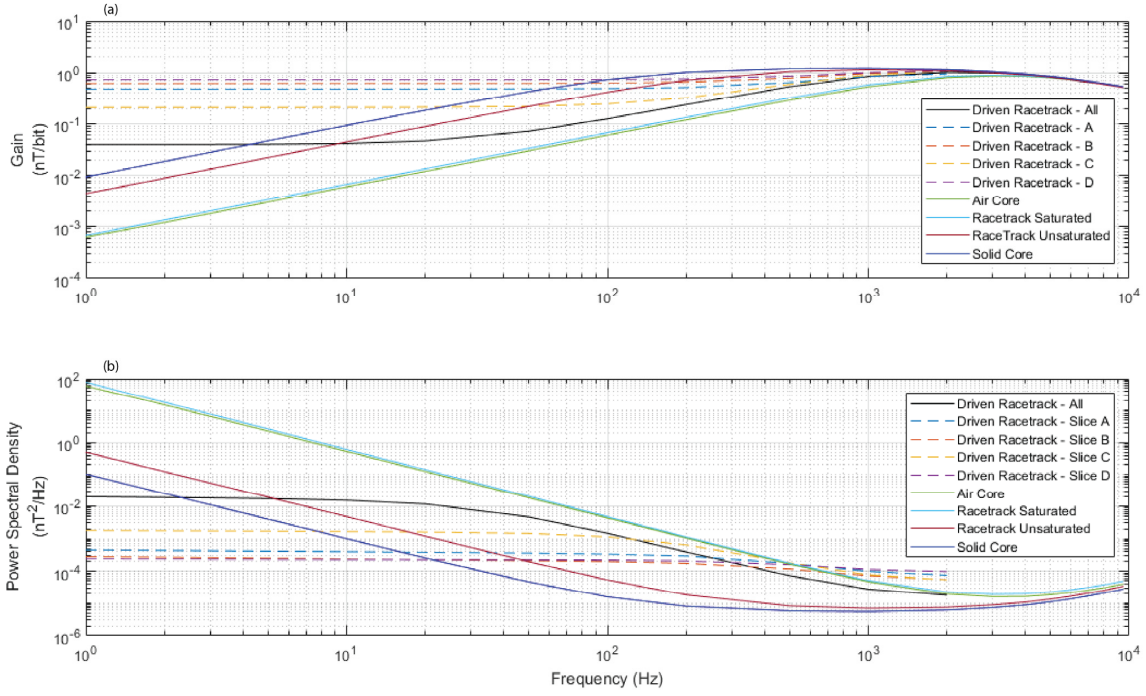

Figure 11: (a) Comparison of frequency dependent gain for various hybrid and standard search coil configurations. (b) Comparison of power spectral density noise floor for the various search coil configurations.

A standard figure of merit for search coil performance is the power spectral density noise floor of the instrument (Figure 11b) using quiet data taken inside a magnetic shield normalised by the frequency dependent gain. As expected, the solid mumetal core provides the lowest noise followed by the unsaturated racetrack core. The air core and the continuously saturated racetrack core provide the poorest result. The un-sliced hybrid search coil path performs between the solid- and air-core limits as expected. However, the sliced hybrid search coil path performs significantly worse than the air core search coil above ~500 Hz where the search coil gain can be accurately measured without interference from the aliased fluxgate signal.

7 Comparison of Fluxgate and Search coil Effects

Figure 12 compares the sensitivity and noise floor obtained from the hybrid instrument using both the fluxgate reconstruction and the unsliced search coil reconstruction. The fluxgate reconstruction provides essentially flat sensitivity with frequency (Figure 12a) and a superior noise floor at low frequencies (Figure 12b). As expected, the search coil reconstruction is much more frequency dependent and provides modestly superior gain and noise above ~1 kHz. Figure 12 also shows the performance of the same sense coil operated as a traditional search coil with a solid mumetal core to illustrate how much search coil performance is sacrificed by operating it as a hybrid sensor.

Geosci. Instrum. Method. Data Syst. Discuss., https://doi.org/10.5194/gi-2018-29
Manuscript under review for journal Geosci. Instrum. Method. Data Syst.
Discussion started: 19 June 2018

Geoscientific Instrumentation Methods and Data Systems Discussions
Open Access
EGU

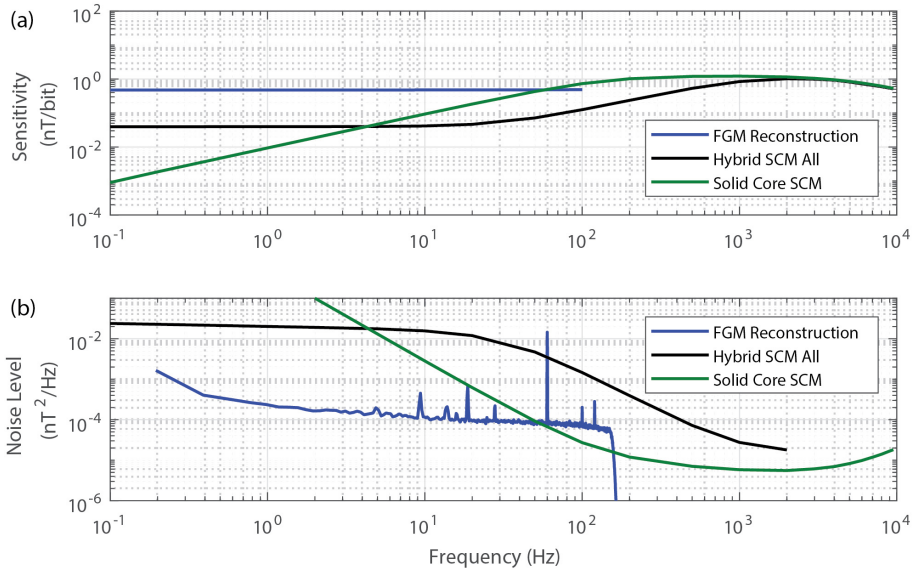

Figure 12: (a) The fluxgate and search coil reconstructions of the hybrid magnetometer data compared to the same sense winding operated as a conventional search coil with a solid core. (a) Frequency dependent sensitivity and (b) instrumental noise floor. The flat response at low frequencies for the search coil reconstruction of the hybrid magnetometer is believed to be an aliasing artefact rather than true instrumental response.

8 Discussion and Conclusions

The presented proof of concept instrument demonstrates how a racetrack sensor can be simultaneously operated as both a fluxgate and a search coil magnetometer. The combination of a racetrack fluxgate core and a long solenoidal sense winding is modestly effective as a search coil magnetometer and the search coil effect can be captured without introducing significant hardware complexity beyond what is already present in a typical fluxgate instrument. The search coil action was found to have significantly different magnetic gain at different phases in the magnetisation cycle of the core. However, slicing the data to use only the phase with highest magnetic gain produced a higher instrumental noise floor than simply using all samples. The best hybrid search coil reconstruction performed roughly four times better (6 dB), in terms of power spectral density noise floor, than an air core with the same sense winding and roughly ten times worse (-10 dB) than the same sense winding paired with a comparably sized solid mumetal core.

It seems likely that the number of turns in the sense winding would need to be increased by roughly an order of magnitude, and the preamplifier gain doubled or quadrupled, to provided search coil performance comparable to that of historical space-based instruments. This proof-of-concept instrument achieves a noise floor of $\sim 3 \times 10^{-5}$ nT^2 Hz^{-1} at 1,000 Hz compared to $\sim 5 \times 10^{-10}$ nT^2 Hz^{-1} for the ~10 cm search coil on MMS and $\sim 3 \times 10^{-11}$ nT^2 Hz^{-1} for the ~40 cm search coil on the Van Allen Probes (Hospodarsky, 2016). The coil and preamplifier design will need to be coupled with careful optimisation of drive frequency, the self-resonance frequency of the coil, and digitiser resolution to exploit the high search coil gain without exceeding the bandwidth of the analog electronics or the digitiser. In particular, the self-resonance of the coil should likely be optimised to align with the

base band search coil bandwidth. Combined with a higher order low-pass anti-alias filter this should improve the search coil performance while preventing interference between the searchcoil and fluxgate actions. It remains to be seen if the sensitivities of the two effects in a hybrid instrument can simultaneously be made operationally useful. It is also possible that with sufficiently high instrumental sensitivity we will discover that the search coil action is contaminated by Barkhausen noise, caused by periodically saturating the core, at a level that limits usefulness of the search coil data. This sensor topology should miniaturize to platforms such a CubeSats where multiple boom-mounted instruments are generally impractical so a single hybrid instrument providing even modest sensitivity from DC to ten kHz could be beneficial.

10 Future Work

The bandwidth of the search coil reconstruction is limited by the fluxgate drive frequency. Moving to a thinner Permalloy foil should allow the racetrack core to be efficiently driven at higher frequencies and enable a wider search coil bandwidth. The fluxgate noise floor still seems to be dominated by the magnetic noise of the core so the number of turns in the sense winding and its self-resonance could likely be optimised with minimal impact on the fluxgate action as long as the bandwidth of the coupled fluxgate drive does not saturate the instrument. Higher resolution digitisation (>16 bit) will likely be required to achieve a competitive search coil noise level given the large analog bandwidth necessary to accommodate the raw fluxgate signal.

Code and Data Availability

Data and source code used in the creation of this paper are available from Miles (2018).

Author Contributions

DMM led the experiment, designed and built the experimental apparatus, executed the experiment, analysed the data, and prepared the manuscript with contributions from all authors. BBN created the magnetic material for the racetrack sensor and designed heat treatment of the racetrack cores. IRM and DKM helped interpret the fluxgate behaviour of the hybrid instrument. DB designed the racetrack core. GH helped interpret the search coil behaviour of the hybrid instrument.

Competing Interests

B. B. Narod operated Narod Geophysics Ltd., which manufactured fluxgate magnetometers until the company ceased production operation in 2008.

Acknowledgements

Work on the project was supported by the Canadian Space Agency under contract 9F063-140909/006/MTB. D. M. Miles was supported by an NSERC PGSD graduate scholarship, faculty start-up funding from the University of Iowa, and an Old Gold Summer Fellowship from the University of Iowa College of Liberal Arts and Sciences. I. R. Mann is supported by a Discovery Grant from Canadian NSERC. The authors wish to thank T. Haluza-DeLay for manufacturing the solenoidal sense winding and Z. Dent for attaching the driving winding to the racetrack core. M. Ciurzynski manufactured and heat-treated the racetrack core and

provided detailed comments on an early version of this manuscript. A. Kale provided comments on an early version of the experiment. J. Larson provided comments on an early version of this manuscript.

References

Acuna, M.: Fluxgate magnetometers for outer planets exploration, IEEE Trans. Magn., 10(3), 519–523, doi:10.1109/TMAG.1974.1058457, 1974.

Angelopoulos, V.: The THEMIS mission, in The THEMIS Mission, pp. 5–34, Springer. [online] Available from: http://link.springer.com/chapter/10.1007/978-0-387-89820-9_2 (Accessed 16 September 2016), 2009.

Gordon, D., Lundsten, R. and Chiarodo, R.: Factors affecting the sensitivity of gamma-level ring-core magnetometers, IEEE Trans. Magn., 1(4), 330–337, doi:10.1109/TMAG.1965.1062987, 1965.

Hinnrichs, C., Pels, C. and Schilling, M.: Noise and linearity of a fluxgate magnetometer in racetrack geometry, J. Appl. Phys., 87(9), 7085–7087, doi:10.1063/1.372939, 2000.

Hinnrichs, C., Stahl, J., Kuchenbrandt, K. and Schilling, M.: Dependence of sensitivity and noise of fluxgate sensors on racetrack geometry, IEEE Trans. Magn., 37(4), 1983–1985, doi:10.1109/20.951028, 2001.

Hospodarsky, G. B.: Spaced-based search coil magnetometers, J. Geophys. Res. Space Phys., 121(12), 2016JA022565, doi:10.1002/2016JA022565, 2016.

Ioan, C., Moldovanu, A., Macovei, C. and Moldovanu, E.: Extension of the frequency range of fluxgate magnetometers, J. Magn. Magn. Mater., 157–158(Supplement C), 567–568, doi:10.1016/0304-8853(95)01145-5, 1996.

Kessel, R. L., Fox, N. J. and Weiss, M.: The Radiation Belt Storm Probes (RBSP) and Space Weather, Space Sci. Rev., 179(1–4), 531–543, doi:10.1007/s11214-012-9953-6, 2013.

Miles, D. M.: Data for A Hybrid Fluxgate and Search Coil Magnetometer Concept Using a Racetrack Core, [online] Available from: https://doi.org/10.25820/t6pr-1551, 2018.

Miles, D. M., Bennest, J. R., Mann, I. R. and Millling, D. K.: A radiation hardened digital fluxgate magnetometer for space applications, Geosci. Instrum. Methods Data Syst., 2(2), 213–224, 2013.

Miles D. M., Mann I. R., Ciurzynski M., Barona D., Narod B. B., Bennest J. R., Pakhotin I. P., Kale A., Bruner B., Nokes C. D. A., Cupido C., Haluza-DeLay T., Elliott D. G. and Milling D. K.: A miniature, low-power scientific fluxgate magnetometer: A stepping-stone to cube-satellite constellation missions, J. Geophys. Res. Space Phys., 121(12), 11,839-11,860, doi:10.1002/2016JA023147, 2016.

Narod, B. B.: The origin of noise and magnetic hysteresis in crystalline permalloy ring-core fluxgate sensors, Geosci. Instrum. Methods Data Syst., 3(2), 201, 2014.

Primdahl, F.: The fluxgate magnetometer, J. Phys. [E], 12(4), 241, 1979.

Primdahl, F., Nielsen, O. V., Petersen, J. R. and Ripka, P.: High frequency fluxgate sensor noise, Electron. Lett., 30(6), 481–482, 1994.

Ripka, P.: Improved fluxgate for compasses and position sensors, J. Magn. Magn. Mater., 83(1), 543–544, doi:10.1016/0304-8853(90)90618-Z, 1990.

Ripka, P.: Race-track fluxgate sensors, Sens. Actuators Phys., 37–38(Supplement C), 417–421, doi:10.1016/0924-4247(93)80071-N, 1993.

Ripka, P.: Race-track fluxgate with adjustable feedthrough, Sens. Actuators Phys., 85(1), 227–231, doi:10.1016/S0924-4247(00)00394-0, 2000.

Ripka, P., Primdahl, F., Nielsen, O. V., Petersen, J. R. and Ranta, A.: A.c. magnetic-field measurement using the fluxgate, Sens. Actuators Phys., 46(1), 307–311, doi:10.1016/0924-4247(94)00911-Z, 1995.

Wallis, D. D., Miles, D. M., Narod, B. B., Bennest, J. R., Murphy, K. R., Mann, I. R. and Yau, A. W.: The CASSIOPE/e-POP Magnetic Field Instrument (MGF), Space Sci. Rev., 189(1–4), 27–39, doi:10.1007/s11214-014-0105-z, 2015.